Available online at www.sciencedirect.com
ScienceDirect
Atmospheric Environment 40 (2006) S552–S562
ATMOSPHERIC ENVIRONMENT
www.elsevier.com/locate/atmosenv

Impacts of ozone precursor limitation and meteorological variables on ozone concentration in São Paulo, Brazil

Odón R. Sánchez-Ccoyllo, Rita Yuri Ynoue, Leila Droprinchinski Martins, Maria de Fátima Andrade*

Department of Atmospheric Sciences, Institute of Astronomy, Geophysics and Atmospheric Sciences, University of São Paulo, Rua do Matão, 1226, Cidade Universitaria, São Paulo, SP 05508-900, Brazil

Received 30 July 2005; received in revised form 17 February 2006; accepted 25 April 2006

Abstract

Ozone concentrations in the heavily polluted metropolitan area of São Paulo (MASP), in Brazil, frequently exceed established international standards. This study aims to describe the impact that three meteorological variables (mixing height, wind speed and air temperature) on the ozone concentration, as well as reactive hydrocarbon (RHC) limitation and nitrogen oxide (NO_x) limitation, have on ozone formation in the area. To achieve these objectives the California Institute of Technology (CIT) Eulerian air quality model was applied combined with the same methodology described in Baertsch-Ritter et al. [2004. Atmospheric Chemistry and Physics 4, 423–438] In addition, NO_x and RHC emission inventory reductions were used to evaluate their sensitivities in the CIT model. A simulation of an episode occurring in the MASP on 22 August 2000, when a peak ozone level of 127 ppbv was recorded, is presented. In the CIT model results for the base case, primary pollutant concentrations and ozone concentrations are in good agreement with the measured data. In addition, changes in mixing height, wind speed and air temperature input files have the greatest effect on peak ozone in the MASP, and the isolated effect of RHC emission inventory reduction leads to 26% lower ozone levels than in the base case. Based on the results of this study, we can conclude that with reduction of RHC emission could provide the best scenario for promoting lower ozone concentrations in the MASP.

Keywords: Photochemical model; Urban air pollution; Emission inventory; Meteorological sensitivity; RHC/NO_x limitation

1. Introduction

The metropolitan area of São Paulo (MASP) is a highly industrialized area in South America. Its automotive fleet now exceeds 7.8 million vehicles (CETESB, 2005) and is the main source of air pollutant emissions. The MASP presents an unconventional mixture of vehicle types, which use a variety of fuels, including oxygenated blends such as gasohol (gasoline with 22% alcohol) and pure ethanol (used in the light-duty fleet only) (CETESB, 2001). As a fuel for motor vehicles, ethanol produces less carbon monoxide (CO) than does gasoline but results in greater emission of aldehydes (especially acetaldehyde), giving the urban smog problem a unique photochemical profile.

*Corresponding author. Fax: +55 11 3818 4714.
E-mail address: mftandra@model.iag.usp.br (M. de Fátima Andrade).

1352-2310/$ - see front matter © 2006 Elsevier Ltd. All rights reserved.
doi:10.1016/j.atmosenv.2006.04.069

Emission of the NO–NO_2 combination (NO_x) and of reactive hydrocarbons (RHCs) concurrently with high radiation and temperature leads to frequent elevations in ozone concentrations in the MASP (Massambani and Andrade, 1994). Ozone concentrations frequently exceed the 1-h standard of 82 ppbv, indicating a serious health problem in the MASP (Saldiva et al., 1995; Souza et al., 1998). For example, in the year 2000, the 1-h ozone standard was exceeded in the MASP on 65 days. Surface ozone concentrations are controlled not only by in situ formation, but also through pollutant transport, both of which are dictated by the prevailing meteorological conditions (Biswas and Rao, 2001). The RHC and NO_x limitation characteristics of an air parcel vary dynamically with transport, dispersion, dilution, and photochemical aging (Biswas and Rao, 2001). Because photochemical models are being used in a regulatory setting, it is important to assess the variability in the response of the modeling system to various emission control strategies.

In the MASP, several studies analyzing the influence of meteorological conditions on measured air pollution have been conducted (Orsini et al., 1986; Andrade et al., 1994; Castanho and Artaxo, 2001; Montero et al., 2001; Sánchez-Ccoyllo and Andrade, 2002; Landulfo et al., 2003; Ynoue and Andrade, 2004; Sánchez-Ccoyllo et al., 2006). However, there is little data regarding the effects of RHCs and NO_x sensitivity on ozone production on meteorological variability.

The objectives of this study were: (i) to describe the effect that mixing height, wind speed and air temperature on the ozone concentration; and (ii) RHC limitation and NO_x limitation have on ozone formation during a typical pollution episode, using the California Institute of Technology (CIT) photochemical air quality model. By employing the methodology developed by Baertsch-Ritter et al. (2004), this study may contribute to a better understanding of how meteorological variables influence ozone formation. Baertsch-Ritter et al. (2003) reported that the ozone plume formation is critically dependent on the height of the mixing layer and its diurnal development and on the wind speed.

The most serious errors in photochemical modeling result from the input of unrealistic meteorological and emissions data (Russel and Dennis, 1988). Input files should be considered valid only after a careful evaluation of the model results with regard to a wide range of measured values. It is widely held that simulations, when modeled ozone concentrations are compared to measured data, are representative of the process. However, this is not entirely correct since it is well known that various RHC vs. NO_x ratios can lead to identical quantities of ozone formation. As a consequence, even if ozone formation is modeled correctly, the model might indicate the need for ozone control strategies that are inappropriate. Unrealistic meteorological input parameters could also hinder the accuracy of predicted ozone formation.

2. Area of investigation

Fig. 1 shows the area of investigation and the model domain: the city of São Paulo and 38 surrounding cities, together forming the MASP, which is considered a megacity, with a population of approximately 18 million inhabitants and is situated in southeastern Brazil. The MASP is among the five largest metropolitan areas in the world. In all of these megacities, human activities have an enormous impact on air quality and on the health of the population (Saldiva et al., 1995; Braga et al., 2001).

2.1. Experimental sites

The experimental sites are depicted in Fig. 1. The downtown site (23°33′S, 46°45′W, denoted by a @ in Fig. 1) is on a plateau at approximately 750 m above sea level (asl), 60 km northwest of the South Atlantic Ocean, and is surrounded by mountains of approximately 1200 m in height (Nair et al., 2004). The Agua Funda (AF) site (23°39′S, 46°37′W) is a climatological station operated by the Institute of Astronomy, Geophysics and Atmospheric Sciences (IAG) of the University of São Paulo (USP) and is situated approximately 16 km southeast of downtown. The large AF area features abundant vegetation and contains one of the last remaining tracts of Mata Atlântica (Atlantic rainforest). Local anthropogenic sources have only a minimal impact on the area (Montero et al., 2001). There are no industrial or commercial operations in the immediate vicinity of the AF site. However, pollutant contributions from the city of Cubatão, the largest industrial park in Latin America, may be found in its atmosphere. Presenting various sources of emission, the Cubatão (CB) site is located on the Atlantic coast (23°52′50″S, 46°25′00″W), approximately 44 km southeast of the São Paulo city center and 20 km southeast of

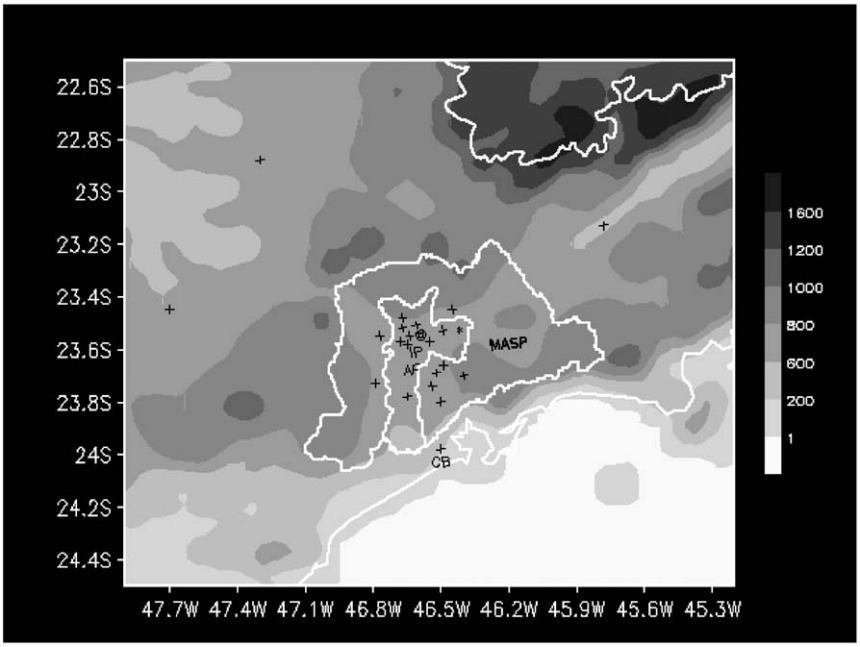

Fig. 1. Modeling domain and monitoring stations. Shaded gray areas represent topography altitudes asl. Each + denotes an air quality monitoring station operated by CETESB. * Represents the São Miguel Paulista monitoring station. @ denotes the downtown São Paulo area. IP (Ibirapuera Park) and CB (Cubatão) represent SODAR locations. AF (Agua Funda) represents the climatological station operated by the University of São Paulo.

the AF site (Fig. 1). The area lies between the ocean and the Serra do Mar mountain range (700–1200 m asl). High levels of air pollution are particularly damaging to the vegetation, which is Atlantic rainforest. A Doppler sound detection and ranging (SODAR) system operated by the IAG-USP is located at the CB site (Nair et al., 2004). The Ibirapuera Park (IP) site is located about 10 km southeast of downtown (23°34′55″S, 46°39′25″W). A major highway with heavy vehicle traffic fueled by gasohol, diesel, and ethanol influences the sampling of ozone concentrations (Alonso et al., 1997). At this site, there is also a Doppler SODAR system, operated by the *Companhia de Tecnologia de Saneamento Ambiental* (CETESB, Environmental Technology and Cleanup Agency) of the state of São Paulo. To describe the mixing height on the plateau and on the coast, the modeled data were compared to the experimental data obtained from SODAR readings.

3. Meteorological conditions

The synoptic conditions of the pollution episode on 22 August were dominated by the South Atlantic High Pressure, a high-pressure system centered over the Atlantic Ocean and extending into the continent over southeastern Brazil. This created conditions favorable for greater photo-oxidant formation (Sánchez-Ccoyllo and Andrade, 2002). The synoptic situation, together with its interaction with local circulation, influences airflow, which plays an important role in pollutant transport in all seasons (Silva Dias et al., 1995, Silva Dias and Machado, 1997). On the day in question, clear skies predominated over the MASP, with prevailing northeasterly winds and high temperatures. At the AF climatological station, a maximum temperature of 29.4 °C was recorded. Based on data collected at AF the average temperature was 19.7 °C, the average relative humidity was 53%, and the average wind speed was relatively low (0.8 m s^{-1}).

4. Model description

This study employed the CIT urban airshed model, which is an Eulerian photochemical model developed jointly by the California Institute of Technology and Carnegie Mellon University. McRae et al. (1982), McRae and Seinfeld (1983), Russell et al. (1988) and Harley et al. (1993) give detailed descriptions of the CIT model.

The Eulerian grid-based CIT urban airshed model describes the formation and transport of chemically reactive species in the turbulent planetary boundary layer, including the formation of ozone and peroxyacetyl nitrate (PAN). The model consists of three basic modules: the meteorological module, the chemistry module and the emission inventories module (including spatial and temporal distribution). The chemistry module evaluates three basic types of chemical species: explicit organic and inorganic species and organic species lumped according to the reactivity of compounds. A detailed description of the model, including a list of recent enhancements and an evaluation of its performance, is presented in Harley et al. (1993).

The model employs the 1999 California Statewide Air Pollution Research Center (SAPRC99) photochemical mechanism developed by Carter (2000a, b). In the present study, this mechanism was expanded to include, explicitly, the chemistry of methane, methanol, ethanol, isoprene, hydrogen peroxide, and sulfur dioxide. Methyl tertiary butyl ether emissions were not included since this fuel is not used in the MASP.

Solar radiation is an important parameter in photochemical kinetics. Diurnal eddy diffusion coefficients are parameterized according to total solar radiation and wind velocity. Photolysis rate coefficients are based on theoretical calculations of the solar flux in the spectral band of interest, and can be corrected by real measurements (McRae et al., 1982). In order to estimate the dry deposition fluxes, the model calculates, initially, the maximum deposition velocity for each grid square according to Russell et al. (1988). This velocity is the same for all of the species, assuming that the surface acts as a perfect sink for the deposition pollutant. The dry deposition velocity for each species is calculated as a function of the maximum deposition velocity and a surface resistance term that depends on the surface type and the solar radiation flux. The surface resistance is specified for each chemical species and the various land-use types. In this simulation, the deposition module was not activated.

4.1. Model domain

Three-dimensional Eulerian air quality model calculations were performed for the 22 August 2000 episode within the modeling domain illustrated in Fig. 1. The simulations were performed for a 60×30 horizontal grid with 5 km × 5 km resolution and five vertical layers. The layer tops were found at 77, 308, 616, 1342 and 2200 m above ground level (agl). The total modeling domain included 9000 cells, 6500 of which were within the computational domain. The CIT model features for the MASP are described in more detail by Ulke and Andrade (2001) and by Andrade et al. (2004).

4.2. Meteorology

The CIT model requires five meteorological input files: mixing depth, three-dimensional wind, surface temperature, absolute humidity, and solar radiation scaling. In the present study, meteorological data input for the base case was determined from Doppler SODAR, surface meteorological instruments and model-derived values. The Doppler SODAR located at the CB site is a phased-array version (REMTECH PA-2), which provides data for heights at 50-m intervals from 50 to 1500 m asl, measured every 15 min (Nair et al., 2004).

In the present study, the regional atmospheric modeling system (RAMS), a prognostic (dynamic) meteorological model (Cotton et al., 2003; Pielke et al., 1992), output was used to create input for the CIT model (Lyons et al., 1995; Pielke and Uliaz, 1998; Biswas and Rao, 2001). The meteorological and photochemical models had the same horizontal resolution. The RAMS was run with variable resolution ranging from 60 to 800 m in vertical height and with a 1-h time resolution. The RAMS model features for the MASP are described in more detailed by Silva Dias and Machado (1997) and Sánchez-Ccoyllo et al. (2006). Modeling of the high horizontal resolution of the atmospheric circulations was performed for the period from 20 to 24 August based on data obtained from the RAMS data assimilation module. From the coarse resolution analysis (1.875°) provided by the *Centro de Previsao de Tempo e Estudos Climaticos/Instituto Nacional de Pesquisas Espaciais* (CPTEC/INPE, Center for Weather Prediction and Climate Studies/National Space Research Institute), the assimilation system generated the high-resolution fields with the appropriate boundary conditions (topography, vegetation, etc.). Every 6 h, the latest CPTEC analysis was fed into the data assimilation module (Cavalcanti et al., 2002).

4.3. Emissions

Emission inventories of total RHCs, CO, NO_x, sulfur oxides (such as SO_2) and particulate matter

with aerodynamic diameters less than 10 μm (PM_{10}) were compiled for the year 2000 (CETESB, 2001). These inventories were spatially and temporally distributed throughout the MASP and adjusted by a factor of 1.3 (for CO, SO_2 and RHCs) and by a factor of 0.9 (for NO_x) based on the analysis of ambient ratio measurements of CO, NO and RHC made by CETESB (2001). The species used to represent the organic emissions were: acetone; alkane group 1; alkane group 2; alkane group 3; aromatics 1; aromatics 2; aromatic aldehydes; butadiene; benzene; acetaldehyde; ethanol; formaldehyde; isoprene; ketones; methanol; olephines 1; olephines 2 and remaining C_3 + aldehydes. The species in SAPRC99 are grouped by reactivity of the compounds. These compounds were scaled proportionally according to ambient measurements made by CETESB (Colón et al., 2001) and by the IAG-USP Laboratory of Atmospheric Processes (Martins et al., 2004).

4.4. Initial and boundary conditions

Initial and boundary conditions were based on pollutant concentrations measured at CETESB air quality stations (CETESB, 2001). Hourly concentrations of routinely monitored gas phase pollutants (ozone, NO, NO_2, SO_2, CO and RHCs) were interpolated for initial and surface boundary conditions based on the weighted average procedure described by Goodin et al. (1979). The structure of the CIT model is presented in Fig. 2.

5. Results and discussion

The base case for this study was calculated using the meteorological conditions and emissions described in Sections 4.2 and 4.3. The results of the base case are presented in Fig. 3. In this figure, vertical bars indicate the standard deviation of the pollutants concentrations measured at the air quality stations in the MASP. Simulated primary pollutant concentrations for the MASP are in good agreement with the average observed values except for some discrepancies in NO values, mainly during the night. The model adequately simulated the diurnal ozone variations and concentrations. The ozone concentrations were highest near the coast (Fig. 4a), indicating that ozone precursors emitted in the MASP are transported to other regions distant from the sources. Since NO_x concentrations inside the MASP are high, ozone peaks are typically found some distance downwind of the sources, where there are no monitoring stations. Other MASP studies have also shown that pollution is exported to other regions (Ulke and Andrade, 2001).

The aim of this study is to analyze the influences of meteorological variables individually. The influences of mixing height, wind speed, and air

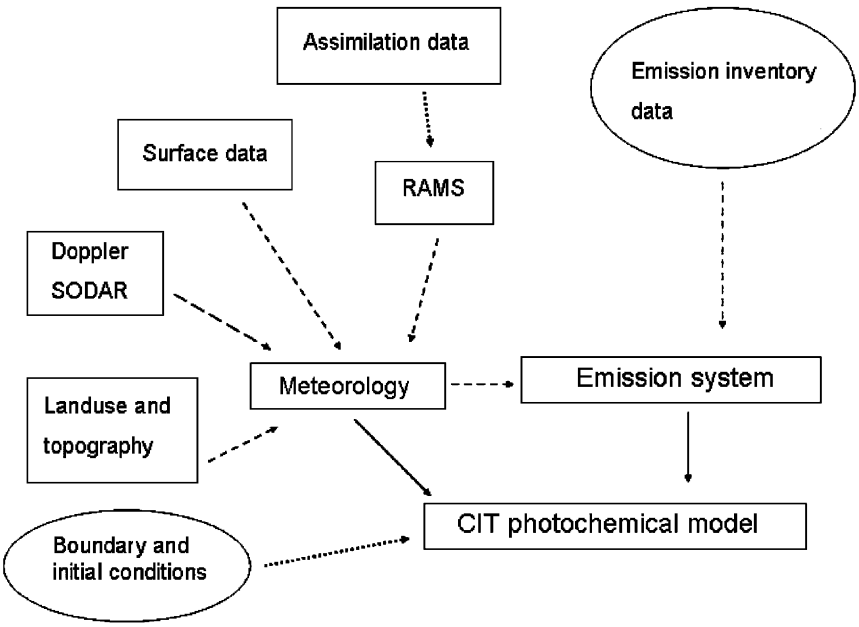

Fig. 2. CIT air quality model with the emissions and meteorological module systems.

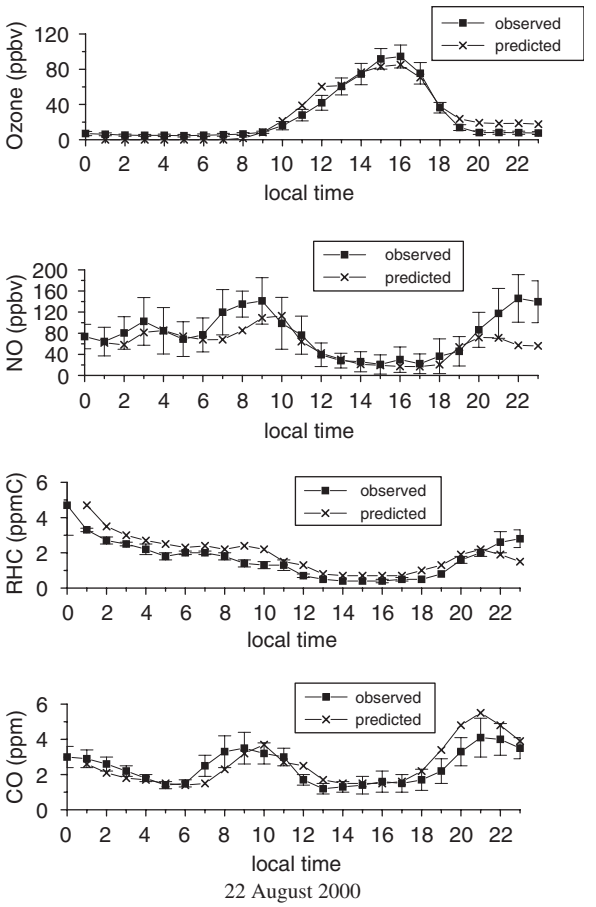

Fig. 3. Measurement of various species on 22 August 2000 in the MASP, in comparison with base case model results (lowest layer). Vertical bars indicate the standard deviation of the measured pollutants concentrations in the air quality stations.

temperature were evaluated and designated A, B and C cases, respectively. Although the radiation intensity is important for ozone formation it was not evaluated, since there are not available hourly data for this area.

Table 1 presents detailed information regarding the cases. Within one case, different variations were simulated. The range of variations was mostly within the variability that can occur in this region on days with conditions that favor high ozone formation. In the A1 case, the original mixing height for 22 August was multiplied by a factor of 1.35, as opposed to a factor of 1.65 for the A2 case. At 1500 LT, the mixing height in the MASP base case was 1200 m agl, compared to 1600 and 2000 m for cases A1 and A2, respectively. For the B cases, the wind speed was higher than in the base case by a factor of 1.5 (B1) and 2.0 (B2). To increase the air temperature (T) by 2 °C, the original temperature field of the base case (BC) was changed by adding 2 °C in each grid cell. So, in scenarios C1–C4, the original T field was varied with a ΔT of −4,−2, 2 and 4 °C.

The production of ozone was RHC-limited downwind of MASP and slightly NO_x-limited in the surroundings (Fig. 4b). In addition RHC or NO_x reductions scenarios were modeled for each of the meteorological variables variations. In these scenarios, anthropogenic RHC or NO_x emissions were individually reduced by 40%. The difference between ozone concentrations for these two models runs yields the ozone limitations (Baertsch-Ritter et al., 2004) (Fig. 4b):

$$\text{Ozone limitation } (O_3\,\text{lim}) = O_3(-40\%\,\text{RHCanthrop.}) - O_3(-40\%\,NO_x),$$

where RHCanthrop represents the RHCs derived from vehicular emissions. The 40% ratio was determined by calculating the ambient ratio of RHC (ppbC) to NO_x (ppb) in the atmosphere of the MASP. The average and standard deviations of RHC/NO_x ratios, as measured by CETESB from 0700 to 0900 local time (LT)—when there is less photochemical activity but great output by the sources—at the downtown site, were 7.0 and 2.9, respectively. Therefore the reduction of 40% (equivalent to the standard deviation) in emissions reflects situations that can be occurring in MASP.

It has been proposed that NO_x limited be defined as $O_3\text{lim} > 0$ ppbv, and RHC limited as $O_3\text{lim} < 0$ ppbv. Therefore, in the computational domain, higher O_3lim indicates higher NO_x sensitivity and lower O_3lim indicates higher RHC sensitivity (Baertsch-Ritter et al., 2004, Lam et al., 2005).

The presented CIT model results are discussed for 22 August at 1500 LT, when the increase in photooxidant production was observed. This particular day and time cannot be regarded as generally representative for this region but it is a good example of an ozone episode inside and in the vicinities of MASP. In order to quantify the CIT model response to the meteorological variations, averages were calculated for MASP (8000 km^2, Fig. 1) and within the plume (25 km^2), which included the highest modeled ozone concentrations. Table 1 shows the average ozone concentration for the BC and the ozone levels obtained in both reduction scenarios for the surface downwind plume and MASP regions. The individual effect of RHC reduction led peak ozone concentrations to drop to

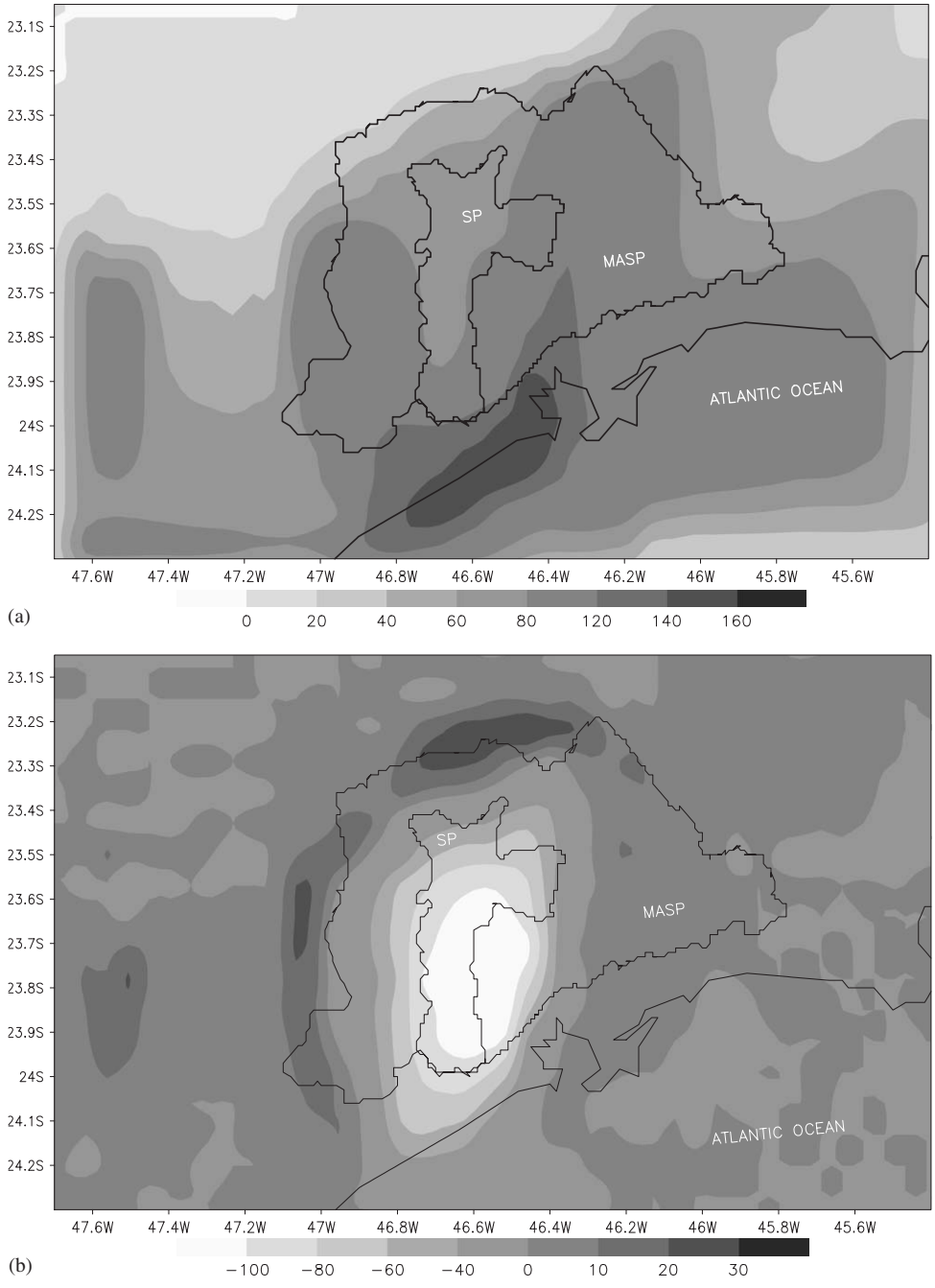

Fig. 4. Modeled values for the base case (BC) at 1500 LT: (a) ozone concentration; (b) ozone limitation.

62.7 ppbv in the MASP (26% lower than the base case value of 85 ppbv) and to 136 ppbv (13% lower than the base case value of 157 ppbv) in the urban plume (Table 1). Figs. 4a and b show the photochemical computational domain for ozone concentration and O_3lim in the base case. The plume concentrations of ozone were highest (157 ppbv) (Fig. 4a), and the formation of ozone was strongly RHC-limited in the MASP emission region (Fig. 4b), where $O_3\text{lim} < -100$ ppbv. The production of ozone also was RHC-limited downwind of MASP, where O_3lim was -40 ppbv. In the MASP suburbs, however, ozone was limited by NO_x ($0\ \text{ppbv} < O_3\text{lim} < 30$ ppbv).

5.1. Case A: mixing height

The changes of mixing height led to lower ozone concentrations in the plume and in the MASP. When the mixing height was increased from 1200 to 2000 m, the modeled ozone peak was 135 ppbv for the plume (14% lower than the base case value of 157 ppbv) and 61 ppbv for the MASP (29% lower than the base case value of 85 ppbv). The ozone reduction is due primarily to dilution of primary emissions into a larger volume.

The combined effect of RHC emission inventory reduction by 40% and higher mixing height (case A2) led ozone concentrations to drop to 48 ppbv in the MASP and 125 ppbv in the plume, compared to 85 and 157 ppbv, respectively, for the base case (Table 1).

In Table 2, the entire computational domain is taken into account, presenting the relative numbers of grid cells when the ozone is limited by NO_x or by RHC (Baertsch-Ritter et al., 2004). These results were obtained from simulations in which NO_x and RHC emission inventory were reduced by 40% in relation to the base case and the two meteorological variables were varied. In Table 2, it can be seen that the number of NO_x-limited and RHC-limited grid cells decreased when mixing height increased. However, the number of RHC-limited grid cells decreased more sharply, to 27%, compared to 35% for the base case.

Table 1
Compilation of mean ozone concentrations in the MASP experimental areas and in the plume for the A- B- and C-case variations valid for 22 August 2000 at 1500 LT

Variation		O_3		O_3 (−40% RHC)		O_3 (−40% NO_x)	
		Plume	MASP	Plume	MASP	Plume	MASP
Mixing height (m agl)							
BC	1200	157	85	136	63	180	149
A1	1600	149	66	134	51	170	106
A2	2000	135	61	125	48	160	93
Wind speed (increase)							
BC	*1	157	85.1	136	63	180	149
B1	*1.5	146	40	145	30	200	78
B2	*2	125	20	95	17	180	39
ΔT (°C)							
C4	4	180	101	154	72	205	177
C3	2	160	93	145	67	189	163
BC	0	157	85	136	63	180	149
C2	−2	145	78	125	58	165	136
C1	−4	125	70	120	54	150	125

Mean average ozone concentrations are also given for the model runs involving 40% reductions in NO_x or anthropogenic RHC emissions. BC = base case.

Table 2
Percentages of NO_x- and RHC-limited grid cells throughout the computational domain for the base case and for A, B, C1 and C4 cases valid for 1500 LT

	Description	NO_x-limited area (%)	RHC-limited area (%)	O_3lim = 0
BC	Emission	53	35	12
A2	Mixing height at 2000 m agl	51	27	22
A1	Mixing height at 1600 m agl	51	31	18
B1	Wind speed increased by 1.5	53	27	20
B2	Wind speed increased by 2.0	49	30	21
C1	$\Delta T = -4$C	49	35	16
C4	$\Delta T = 4$C	55	31	14

BC = base case.

5.2. Case B: wind speed

Also, Table 1 shows the effect that changing the wind speed had on ozone concentrations. Behavior similar to that of mixing height was observed when wind speed was increased. Ozone concentrations decreased in both regions, especially in the MASP (77% at 1500 LT; Table 1). Higher wind speeds promote the dispersion of ozone precursors and thus decrease ozone concentrations.

In Table 2, the relative numbers of NO_x limitation ($O_3\text{lim} > 0$) and RHC limitation ($O_3\text{lim} < 0$) grid cells are presented for B cases (in which wind speeds were changed). Table 2 shows that the higher wind speeds employed in case B2 reduced the RHC-limited area to 30%, compared to 35% for the base case, and the corresponding NO_x-limited area was reduced from the 53% seen in the base case to 49% (Table 2). Therefore, both RHC- and NO_x-sensitive areas shrank in size.

In these CIT model simulations, enhanced wind speeds are indicative of greater dilution of polluted plumes, as has been shown by Biswas and Rao (2001) and Baertsch-Ritter et al. (2004). Baertsch-Ritter et al. (2004) reported that peak ozone levels were 15% lower when the wind speed was doubled. In the current study, doubling the wind speed (case B2) led to a 20% reduction in peak ozone levels. In this case, however, the wind speed was multiplied by 1.5 or 2.0 at all grid points for the whole day, whereas Baertsch-Ritter et al. (2004) increased (doubled) the observed wind speed only during the morning hours.

The combined effect of RHC emission inventory reduction by 40% and increased wind speed (case B2) led ozone concentrations to drop to 17 ppbv in the MASP (81% lower than the 85 ppbv calculated for the base case) and 95 ppbv (40% lower than the 157 ppbv base case value) in the plume (Table 1).

5.3. Case C: temperature

The positive variations in air temperature ($\Delta T = 2$ and 4 °C) led to higher ozone concentrations in the plume and in the MASP, while negative ΔT generated lower ozone concentrations in both places (Table 1). When the air temperature was increased by 4 °C (from 28 to 32 °C), the modeled ozone peak reached 180 ppbv concentration in the plume (15% higher than the base case value of 157 ppbv) and 101 ppbv in the MASP (18% higher than the base case value of 85 ppbv). These results are expected due to the temperature dependence of the constant rate of reactions.

6. Summary and conclusions

The CIT model results show that changes in mixing height, wind speed and air temperature input files have the greatest effect on peak ozone levels. Hence, realistic meteorological input is necessary for an appropriate simulation of the chemistry in the modeling domain.

Table 2 shows the percentages of NO_x- and RHC-limited area for the A, B, C1 and C4 cases. The variations applied fall within the realm of possible wintertime meteorological conditions in the MASP. Here are the principal findings regarding limitation.

These results are consistent with those of Biswas and Rao (2001), in which NO_x and RHC sensitivities were evaluated with a photochemical model using hypothetical emission reductions and the RHC- and NO_x-sensitive regimes were influenced by the differences in the meteorological fields.

Based on the results of the present study, we can conclude that the reduction of RHC emission inventory by 40% creates the best situation for promoting lower ozone concentrations in the MASP. Therefore, reducing RHC emissions is recommended for the MASP. However, RHC reactivity rates vary, and it is important to determine which RHCs should be reduced in order to better control ozone levels in the MASP. Any policy changes aimed at ozone control must take into account the RHC/NO_x ratio in MASP. Further studies are needed in order to arrive at a more appropriate description of the emission inventory and of RHC reactivity.

Acknowledgements

The authors are grateful to the *Fundação de Amparo à Pesquisa do Estado de São Paulo* (FAPESP, Foundation for the Support of Research in the State of São Paulo) for funding this study (Grant no. 02/09060-1) and to the São Paulo state *Companhia de Tecnologia de Saneamento Ambiental* (CETESB, Environmental Technology and Cleanup Agency) for providing the trace gas measurements and meteorological SODAR data at the Ibirapuera Park research site. The authors wish to express their gratitude to Mr. Jefferson Boyles for reviewing the manuscript.

References

Alonso, C.D., Martins, M.H.R.B., Romano, J., Godinho, R., 1997. São Paulo aerosol characterization study. Journal of the Air and Waste Manage Association 47, 1297–1300.

Andrade, F., Orsini, C., Maenhaut, W., 1994. Relation between aerosol sources and meteorological parameters for inhalable atmospheric particles in São Paulo city, Brazil. Atmospheric Environment 28 (14), 2307–2315.

Andrade, M.F., Ynoue, R.Y., Harley, R., Miguel, A.H., 2004. Air-quality model simulating photochemical formation of pollutants: the São Paulo Metropolitan Area, Brazil. International Journal Environment and Pollution 22 (4), 460–475.

Baertsch-Ritter, N., Prevot, A.S.H., Dommen, J., Andreani-Aksoyoglu, S., Keller, J., 2003. Model study with UAM-V in the Milan area (I) during PIPAPO: simulations with changed emissions compared to ground and airborne measurements. Atmospheric Environment 37, 4133–4147.

Baertsch-Ritter, N., Keller, J., Dommen, J., Prevot, A.S.H., 2004. Effects of various meteorological conditions and spatial emission resolutions on the ozone concentration and ROG/NO_x limitation in the Milan area (I). Atmospheric Chemistry and Physics 4, 423–438.

Biswas, J., Rao, S.T., 2001. Uncertainties in episodic ozone modeling stemming from uncertainties in the meteorological fields. Journal of Applied Meteorology 40, 117–136.

Braga, A.L.F., Saldiva, P.H.N., Pereira, L.A.A., Menezes, J.J.C., Conceição, G.M.S., Lin, C.A., Zanobetti, A., Schwartz, J., Dockery, D.W., 2001. Health effects of air pollution exposure on children and adolescents in Sao Paulo, Brazil. Pediatric Pulmonology 31, 106–113.

Carter, W.P.L., 2000a. Implementation of the SAPRC-99 chemical mechanism into the models-3 framework. Report to the United States Environmental Protection Agency. January, 29.〈http://pah.cert.ucr.edu/~carter/reactdat.htm〉.

Carter, W.P.L., 2000b. Documentation of the SAPRC-99 chemical mechanism for VOC reactivity assessment. Final Report to California Air Resources Board Contract No. 92-329, and (in part) 95-308, May 8. 〈http://pah.cert.ucr.edu/~carter/reactdat.htm〉.

Castanho, A.D.A., Artaxo, P., 2001. Wintertime and summertime São Paulo aerosol source apportionment study. Atmospheric Environment 35, 4889–4902.

Cavalcanti, I.F.A., Marengo, J.A., Satyamurty, P., Nobre, C.A., Trosnikov, I., Bonatti, J.P., Manzi, A.O., Tarasova, T., Pezzi, L.P., D'Almeida, C., Sampaio, G., Castro, C.C., Sanches, M.B., Camargo, L., 2002. Global climatological features in a simulation using the CPTEC-COLA AGCM. Journal of Climate 15 (21), 2965–2988.

CETESB, 2001. Report on the air quality in the Metropolitan Region of São Paulo: CETESB. [Report Series] (In Portuguese). Available at 〈http://www.cetesb.sp.gov.br〉.

CETESB, 2005. Report on the air quality in the Metropolitan Region of São Paulo: CETESB. [Report Series] (In Portuguese). Available at 〈http://www.cetesb.sp.gov.br〉

Colón, M., Pleil, J.D., Hartlage, T.A., Guardani, M.L., Martins, M.H., 2001. Survey of volatile organic compounds associated with automotive emissions in the urban airshed of São Paulo, Brazil. Atmospheric Environment 35, 4017–4031.

Cotton, W.R., Pielke, R.A., Walko, S., Liston, R.L., Tremback, G.E., Jiang, H.C., McAnelly, R.L., Harrington, J.Y., Nicholls, M.E., Carrio, G.G., McFadden, J.P., 2003. RAMS 2001: current status and future directions. Meteorology and Atmospheric Physics 82, 5–29.

Goodin, W.R., McRae, G.J., Seinfeld, J.H., 1979. A comparison of interpolation methods for sparse data: application to wind and concentration fields. Journal Applied Meteorology 18, 761–771.

Harley, R.A., Russell, A.G., McRae, G.J., Cass, G.R., Seinfeld, J.H., 1993. Photochemical modeling of the Southern California air quality study. Enviromental Science and Technology 27, 378–388.

Lam, K.S., Wang, T.J., Wu, C.L., Li, Y.S., 2005. Study on an ozone episode in hot season in Hong Kong and transboundary air pollution over pearl river delta region of China. Atmospheric Environment 39 (11), 1967–1977.

Landulfo, E., Papayannis, A., Artaxo, P., Castanho, A.D.A., Freitas, A.Z., Sousa, R.F., Viera Junior, N.D., Jorge, M.P.M.P., Sánchez-Ccoyllo, O.R., Moreira, D.S., 2003. Synergetic measurements of aerosols over São Paulo, Brazil using LIDAR, sunphotometer and satellite data during the dry season. Atmospheric Chemistry and Physics 3, 1523–1539.

Lyons, W.A., Tremback, C.J., Pielke, R.A., 1995. Applications of the regional atmospheric modeling system (RAMS) to provide input to photochemical grid models for the lake Michigan ozone study (LMOS). Journal of Applied Meteorology 34, 1762–1786.

McRae, G.J., Seinfeld, J.H., 1983. Development of a second-generation mathematical model for urban air pollution. II evaluation of model performance. Atmospheric Environment 17, 501–522.

McRae, G.J., Goodin, W.R., Seinfeld, J.H., 1982. Development of second-generation mathematical model for urban air pollution—I model formulation. Atmospheric Environment 16, 679–696.

Martins, L.D., Andrade, M.F., Vasconcellos, P.C., Pretto, A., Yamazaki, A., Gatti, L.V., Albuquerque, E.L., Tomaz, E., 2004. Ambient levels of volatile organic compounds in the atmosphere of the São Paulo megacity (in Portuguese). XIII Brazilian Meteorology Congress.

Massambani, O., Andrade, M.F., 1994. Seasonal behavior of tropospheric ozone in the São Paulo (Brasil) metropolitan area. Atmospheric Environment 28, 3165–3169.

Montero, L., Vasconcellos, P.C., Souza, S.R., Pires, M.A.F., Sánchez-Ccoyllo, O.R., Andrade, M.F., Carvalho, L.R.F., 2001. Measurements of atmospheric carboxylic acids and carbonyl compounds in São Paulo city, Brazil. Environmental Science and Technology 35, 3071–3081.

Nair, K.N., Freitas, E.D., Sánchez-Ccoyllo, O.R., Silva Dias, M.A.F., Silva Dias, P.L., Andrade, M.F., Massambani, O., 2004. Dynamics of urban boundary layer over São Paulo associated with mesoscale processes, meteorology and atmospheric physics 86 (1–2), 87–98.

Orsini, C., Tabacniks, M., Artaxo, P., Andrade, M.F., Kerr, A.S., 1986. Characteristics of fine and coarse particles of natural and urban aerosols of Brazil. Atmospheric Environment 20, 2259–2269.

Pielke, R.A., Uliaz, M., 1998. Use of meteorological models as input to regional and mesoscale air quality models—limitations and strengths. Atmospheric Environment 32, 1455–1466.

Pielke, R.A., Cotton, W.R., Walko, R.L., Tremback, C.J., Lyons, W.A., Grasso, L.D., Nicholls, M.E., Moran, M.D.,

Wesley, D.A., Lee, T.J., Copeland, J.H., 1992. A comprehensive meteorological modeling system—RAMS. Meteorology and Atmospheric Physics 49 (1–4), 69–91.

Russell, A.G., McCue, K.F., Cass, G.R., 1988. Mathematical modeling of the formation of nitrogen-containing air pollutants. 1. evaluation of an Eulerian photochemical model. Environmental Science and Technology 22 (3), 263–271.

Saldiva, P.H.N., Pope, C.A., Schwartz, J., Dockery, D.W., Lichtenfels, A.J., Salge, J.M., Barone, I., Bohm, G.M., 1995. Air pollution and mortality in elderly people: a time-series study in São Paulo, Brazil. Archives Environmental Health 50, 159–163.

Sánchez-Ccoyllo, O.R., Andrade, M.F., 2002. The influence of meteorological conditions on the behaviour of pollutants concentrations in São Paulo. Environmental Pollution 116, 257–263.

Sánchez-Ccoyllo, O.R., Silva Dias, P.L., Andrade, M.F., Freitas, S.R., 2006. Determination of O3, CO and PM10 transport in the metropolitan area of São Paulo, Brazil through synoptic-scale analysis of back trajectories. Meteorology and Atmospheric Physics 92, 83–93.

Silva Dias, M.A.F., Machado, A.J., 1997. The role of local circulations in summertime convective development and nocturnal fog in São Paulo, Brazil. Bound-Layer Meteorology 82, 135–157.

Silva Dias, M.A.F., Vidale, P.F., Blanco, C.M.R., 1995. Case study and numerical simulation of the summer regional circulation in São Paulo, Brazil. Boundary-Layer Meteorology 74, 371–388.

Souza, M.B., Saldiva, P.H.N., Pope, C.A., Capelozzi, V.L., 1998. Respiratory changes due to long-term exposure to urban levels of air pollution. CHEST 113 (5), 1312–1318.

Ulke, A.G., Andrade, M.F., 2001. Modeling urban air pollution in São Paulo, Brazil: sensitivity of model predicted concentrations to different turbulence parameterizations. Atmospheric Environment 35, 1747–1763.

Ynoue, R.Y., Andrade, M.F., 2004. Size-resolved mass balance of aerosol particles over the Sao Paulo metropolitan area of Brazil. Aerosol Science and Technology 38 (S2), 52–62.